Dalton Transactions

Accepted Manuscript

This is an *Accepted Manuscript*, which has been through the Royal Society of Chemistry peer review process and has been accepted for publication.

Accepted Manuscripts are published online shortly after acceptance, before technical editing, formatting and proof reading. Using this free service, authors can make their results available to the community, in citable form, before we publish the edited article. We will replace this *Accepted Manuscript* with the edited and formatted *Advance Article* as soon as it is available.

You can find more information about *Accepted Manuscripts* in the Information for Authors.

Please note that technical editing may introduce minor changes to the text and/or graphics, which may alter content. The journal's standard Terms & Conditions and the Ethical guidelines still apply. In no event shall the Royal Society of Chemistry be held responsible for any errors or omissions in this *Accepted Manuscript* or any consequences arising from the use of any information it contains.

ROYAL SOCIETY OF CHEMISTRY

www.rsc.org/dalton

Highly Efficient Electrochemiluminescence Based on Pyrazolecarboxylic Metal Organic Framework

Chao Feng,[a] Yu-Heng Ma,[a, b] Duo Zhang,[a] Xue-Jing Li,[a] and Hong Zhao*[a]

A series of transition metal complexes with the ligands 3-pyrazoledicarboxylic acid (H_2L^1) and ethyl 1-(2-ethoxy-2-oxoethyl)-1*H*-pyrazole-3-carboxylate (epzc) have been synthesized. The epzc generated 1-(carboxymethyl)-1*H*-pyrazole-3-carboxylic acid (H_2L^2) by the reaction of hydrothermal *in situ* hydrolysis, using the method of one-pot reaction. Simple mononuclear $[Co(HL^1)_2(H_2O)_2]$ (**1**), $[Ni(L^2)(H_2O)_4]$ (**4**), dinuclear $[Ni_2(L^1)_2(H_2O)_6]\cdot H_2O$ (**2**), $[Cu_2(L^2)_2(H_2O)_4]$ (**5**) and 2D framework $[Cu_2(L^1)_2]_n$ (**3**), $[Co_2(L^2)_2(H_2O)_4]_n$ (**6**) have been isolated. The structures have been established by single-crystal X-ray diffraction, and characterized by FT-IR, thermogravimetric analysis (TGA), PRXD, UV–Vis spectroscopy, and fluorescent spectroscopy. **1**, **2**, **4** and **5** is further assembled to form a supramolecule by hydrogen-bonding interactions and/or $\pi\cdots\pi$ stacking. **3** and **6** possess a 2D network structure that is further interlinked *via* intermolecular hydrogen-bonding interactions. Most importantly, complexes demonstrated highly intense electrochemiluminescence (ECL) in DMF solution.

Introduction

The last decades have testified a rapid growth in the area of metal-organic frameworks (MOFs) owing to their various potential applications, ranging from luminescent, magnetism, catalysis to gas sorption and storage, biomedical utilities.[1, 2] The rational design and synthesis of coordination architectures (discrete and polymeric) with metal ions (or metal clusters) and organic ligands is still at an evolutionary stage with the current focus mainly on understanding the factors to determine the crystal packing.[3] In addition to coordination bonding,[4, 5] some weak interactions,

[a] *School of Chemistry and Chemical Engineering, Southeast University, Nanjing 211189, P.R. China. Email: zhaohong@seu.edu.cn*
[b] *Chia-tai Tianqing Pharmaceutical Group Co. Ltd., Nanjing 210023, PR China.*
Electronic supplementary information for **1**-6 available.

Dalton Transactions Accepted Manuscript

such as hydrogen bonding[6] and $\pi\cdots\pi$ stacking[7] interactions also greatly affect the structures of coordination complexes, and they may link multinuclear discrete subunits or low-dimensional entities into high-dimensional supramolecular networks.

Notwithstanding of their strong presence in traditional complex synthesis, 1*H*-pyrazole based ligands especially containing a flexible backbone are seldom reported in the literature.[8] This is particularly true for photoluminescent networks, one of the most studied branch of MOFs.[9] Especially, the relationship between the structural aspects of MOFs and electroluminescent properties has attracted extensive attention in recent times with the aim of understanding the fundamental factors governing photophysical properties. Despite a plethora of recent literature sources on luminescent MOFs, such networks based on 1*H*-pyrazole based ligands still remain one of the most intriguing yet elusive varieties.[10] Notwithstanding, pyrazole based ligands provide a broad scope of study of functional MOFs.

Flexibility of the ligands is also a key factor during MOF synthesis.[11] A rigid ligand almost invariably leads to an inflexible framework. On the contrary, it is well known that introducing a flexibility in the structure may result some advantages by enhancing its reversible response to the presence or absence of guests.[12] One of the popular ways of introducing flexibility in the network is to incorporate a flexible bridging ligand.[13] The ability of flexible ligands to adopt, depending on the coordination requirement, different conformations *via* bending, stretching, twisting, or rotating when coordinating to the metal center remains the major driving force behind this trend.[14]

More recently, Runde group has strong interests in introducing a flexible carboxyl group to the 1-position of the pyrazole ring. Several intriguing MOFs have been successfully synthesized with pyrazol-1-yl) acetic acid ligand.[15] The researches show that the pyrazole carboxylate ligands have

Dalton Transactions Accepted Manuscript

strong coordination ability and various coordination modes. This prompted scientists to prepare more similar organic ligands to study their coordination features.

Inspired by the aforesaid facts, we have introduced the flexible group carboxymethyl on 1-position of 1*H*-pyrazole-3-carboxylic acid (HL^1) through the reaction of *N*-alkylation enhancing the coordination ability, and obtained ethyl 1-(2-ethoxy-2-oxoethyl)-1*H*-pyrazole-3-carboxylate (epzc). Furthermore, the ester generated 1-(carboxymethyl)-1*H*-pyrazole-3-carboxylic acid (H_2L^2) by the reaction of hydrothermal *in situ* hydrolysis, using the method of one-pot reaction. Moreover, flexible group present in these pyrazole based ligands led to a wide range of conformations which have often turned out to be the structure determining factor by exerting considerable structural influence to form diverse topologies. In continuation to our interest in pyrazole based ligand molecules, we carried out two series of pyrazole based ligands H_2L^1 and (epzc) by reactions hydrothermal *in situ* hydrolysis with the main group metal salts $M(NO_3)_2{\cdot}nH_2O$ (M= Cu, Co and Ni), thus six coordination complexes $[Co(HL^1)_2(H_2O)_2]$ (**1**), $[Ni_2(L^1)_2(H_2O)_6]{\cdot}H_2O$ (**2**), $[Cu_2(L^1)_2]_n$ (**3**), $[Ni(L^2)(H_2O)_4]$ (**4**), $[Cu_2(L^2)_2(H_2O)_4]$ (**5**) and $[Co_2(L^2)_2(H_2O)_4]_n$ (**6**) were isolated. In this article, the synthesis, crystal structures, electroluminescence (ECL) and thermal study of **1**-**6** are described.

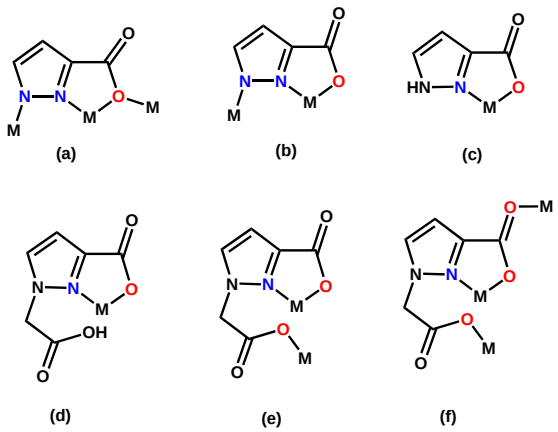

Scheme 1 Coordination modes of H_2L^1 and H_2L^2

Dalton Transactions Accepted Manuscript

Experimental

All reagents were commercial grade materials and used without purification. The building-up process of ligands and complexes were shown in scheme 2. Elemental analyses were performed with a Thermo Quest Flash EA1112 microanalyzer. IR spectra were recorded on a Spectrum One Perkin-Elmer FT-IR spectrophotometer (KBr disc) from 4000 to 400 cm^{-1}. TGA measurements were performed by heating the crystalline sample from 50 to 800 ºC at a rate of 20 ºC min^{-1} in air on a Netzsch STA 409PC differential thermal analyzer. Powder X-ray diffraction (PXRD) was measured on a Rigaku D/MAX 2000 PC X-ray diffraction instrument. The UV–Vis spectrum was recorded on an UV-2450 spectrophotometer. Luminescence spectra for the liquid state samples were investigated with a Horiba Fluoromax-4 fluorescence spectrophotometer. The crystal structure was determined by single crystal diffraction and SHELXL crystallographic software.

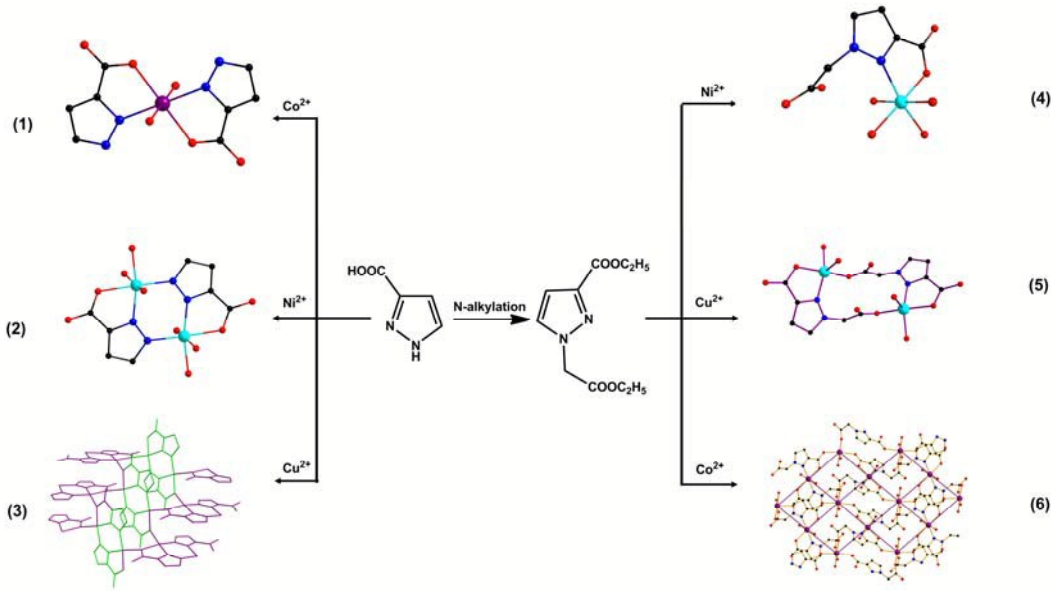

Scheme 2 The building-up process of ligands and complexes **1**-**6**

Preparation of epzc

To solution of ethanol (50 mL) and 3-pyrazolecarboxylic acid (1.112g 10 mmol) at 80 ºC was added concentrated sulfuric acid (2 mL), and after 2 h of stirring the ethyl 1*H*-pyrazole-3-carboxy-

Dalton Transactions Accepted Manuscript

late was obtained (1.350 g, 9.6 mmol, 96%). To 20 mL three-necked round bottomed flask equipped with a refluxing condenser was added 1*H*-pyrazole-3-carboxylate (0.7 g, 5 mmol), ethyl bromoacetate (0.835 g, 0.6 mmol) in 30 mL anhydrous acetone. This suspension was stirred at 60 ºC and the reaction was monitored by TLC. When the 1*H*-pyrazole-3-carboxylate was consumed, the yellow brown reaction mixture was concentrated to dryness. The crude product was purified by column chromatography on silica gel with petroleum ether/ethyl acetate (1/1) as eluent to give the liquid state product epzc in yield of 55% (0.622 g, 2.7 mmol). ^{1}H NMR (DMSO-d_6, 400 MHz): δ 7.60 (d, *J* = 2Hz, 1H), 6.92 (d, *J* = 2Hz, 1H), 5.29 (s, 2H), 4.28-4.22 (m, 2H), 4.15-4.10 (m, 2H), 1.27-1.24 (m, 3H), 1.20-1.16(m, 3H); ^{13}C NMR (DMSO-d_6, 100 MHz): 168.29, 159.50, 139.01, 132.95, 111.87, 61.55, 61.48, 53.77, 14.44, 14.40.

Preparation of $[Co(HL^1)_2(H_2O)_2]$ (1)

$Co(NO_3)_2{\cdot}6H_2O$ (0.0291g, 0.1 mmol) dissolved in water (8mL) was add to test tube and ethyl acetate (5mL) added drop wise, H_2L^1 (0.0112 g, 0.1mmol) dissolved in CH3OH (8mL) was added to the test tube. After 7 days, red block crystals were obtained in about 47% yield based on Co. Anal. Calc. for $C_8H_{10}CoN_4O_6$: (*Mr* = 317.13): C 30.20, H 3.19; N 17.62%. IR (KBr; cm^{-1}): 3203 (s), 1604 (s), 1517 (w), 1496 (m), 1361 (s), 1242 (m), 1179 (w), 1113 (w), 768 (w), 612 (w).

Preparation of $[Ni_2(L^1)_2(H_2O)_6]{\cdot}H_2O$ (2)

$Ni(NO_3)_2{\cdot}6H_2O$ (0.0291 g, 0.1mmol) dissolved in water (8mL) was add to test tube and ethyl acetate (5 mL) was added drop wise, H_2L^1 (0.0112 g, 0.1 mmol) dissolved in CH_3OH (8 mL) was added to the test tube. After 7 days, green block crystals were obtained in about 51% yield based on Ni. Anal. calc for $C_8H_{20}N_4Ni_2O_{12}$: (*Mr* = 481.70): C 19.87, H 4.19; N 11.60%. IR (KBr; cm^{-1}): 3292 (s), 3204 (s), 1606 (s), 1443 (m), 1363 (s), 1243 (m), 1181 (w), 1116 (w), 770 (m), 698 (m).

Dalton Transactions Accepted Manuscript

Preparation of $[Cu_2(L^1)_2]_n$ (3)

A mixture of H_2L^1 (0.0112 g, 0.1 mmol,), $Cu(NO_3)_2{\cdot}3H_2O$ (0.0482 g, 0.2 mmol), and ethanol (15 mL) was put into a Teflon-lined autoclave. The reaction mixture was heated at 120 centigrade for 5 days, followed by slow cooling to room temperature and blue single crystals were collected in about 45% yield based on Cu. Anal. calc for $C_4H_2CuN_2O_2$ (*Mr* = 173.62): C 27.60, H 1.18; N 16.09%. IR (KBr; cm^{-1}): 3426 (s), 3133 (m), 1668 (s), 1334 (s), 1248 (m), 1192 (m), 1147 (s), 779 (s), 625 (m).

Preparation of $[Ni(L^2)(H_2O)_4]$ (4)

A mixture of epzc (0.0226 g, 0.1 mmol,), $Ni(NO_3)_2{\cdot}6H_2O$ (0.0582 g, 0.2 mmol), KOH (0.0112g, 0.2 mmol) and ethanol/H_2O (4/1, 15 mL) was put into a Teflon-lined autoclave. The reaction mixture was heated at 120 centigrade for 5 days, followed by slow cooling to room temperature and green single crystals were collected in about 43% yield based on Ni. Anal. calc for $C_6H_{12}NiN_2O_8$ (*Mr* = 298.87): C 24.02, H 4.18; N 4.60%. IR (KBr; cm^{-1}): 3146 (s) 3084 (s), 1628 (s), 1537 (m), 1391 (s), 1306 (m), 1219 (w), 1082 (w), 980 (w), 782 (m).

Preparation of $[Cu_2(L^2)_2(H_2O)_4]$ (5)

A mixture of epzc (0.0226 g, 0.1 mmol,), $Cu(NO_3)_2{\cdot}3H_2O$ (0.0482 g, 0.2 mmol), KOH (0.0112g, 0.2 mmol) and ethanol/H_2O (4/1, 15 mL) was put into a Teflon-lined autoclave. The reaction mixture was heated at 120 centigrade for 5 days, followed by slow cooling to room temperature and blue single crystals were collected in about 53% yield based on Cu. Anal. calc for $C_{12}H_{16}Cu_2N_4O_{12}$ (*Mr* = 535.37): C 26.85, H 2.30; N 11.91%. IR (KBr; cm^{-1}): 3200 (s) 3113 (s), 1495 (w), 1437 (w), 1396 (s), 1360 (s), 1217 (w), 1088 (w), 827 (w), 784 (m).

Preparation of $[Co_2(L^2)_2(H_2O)_4]_n$ (6)

Dalton Transactions Accepted Manuscript

A mixture of epzc (0.0226 g, 0.1 mmol,), $Co(NO_3)_2 \cdot 6H_2O$ (0.0582 g, 0.2 mmol), KOH (0.0112g, 0.2 mmol) and ethanol/H_2O (4/1, 15 mL) was put into a Teflon-lined autoclave. The reaction mixture was heated at 120 centigrade for 5 days, followed by slow cooling to room temperature and red single crystals were collected in about 53% yield based on Co. Anal. calc for $C_{12}H_{16}Co_2N_4O_{12}$ (*Mr* = 526.15): C 27.30, H 3.08; N 12.13%. IR (KBr; cm^{-1}): 3353 (s) 3125 (s), 1578 (s), 1510 (w), 1439 (s), 1404 (m), 1378 (s), 1084 (w), 808 (w), 783 (m).

Crystal structure determination

Single-crystal X-ray diffraction analyses of **1-6** were carried out on a Bruker SMART Apex CCD diffractometer with graphite-monochromated Mo-Kα radiation (λ = 0.71073 Å) using the ω–θ scan technique at 293 K. The structure was solved by direct methods with SHELXS-97 and refined by full matrix least squares on F^2 with SHELXL-97.[16] All non-hydrogen atoms were refined with anisotropic thermal parameters. Hydrogen atoms were added theoretically and refined with a riding model and fixed isotropic thermal parameters. Detailed data collection and refinements of **1-6** are summarized in Table S1. Selected bond lengths and angles are listed in Table S2. Relevant hydrogen bonding parameters of **1-6** are summarized in Table S3.

Electrochemistry

Electrochemistry was performed with an MPI-A Electrochemical workstation (Xi An, China). All experiments employed a standard three-electrode cell; the reference electrode was a Ag/AgCl electrode, the auxiliary electrode a platinum wire, and the working electrode a glassy carbon electrode (GCE) with a diameter of 1 mm (CV in DMF) (ECL experiments in DMF). The supporting electrolyte was 0.1 M potassium peroxydisulfate ($K_2S_2O_8$), in DMF.

Results and discussion

Dalton Transactions Accepted Manuscript

Structure of $[Co(HL^1)_2(H_2O)_2]$ (1)

Single-crystal X-ray diffraction analysis on selected crystals showed that compound **1** crystallize in the monoclinic crystal system, space group $P2_1/c$. Figure 1a shows a view of structure **1,** the metal atoms are located at the inversion center and are six-coordinate. Co(II) center is bonded to two $(HL^1)^-$ ions at equatorial positions through the chelating carboxylate oxygen O1 and its adjacent pyrazole nitrogen N2, with the Co–O and Co–N bond lengths of 2.0946 (17) and 2.125 (2) Å . These bond lengths are consistent with those found in comparable structures.[17] In addition, Co(II) center is also coordinated to two water molecules at apical positions with a Co–O bond length of 2.0866 (19) Å, which is stronger compared to those in compounds of a similar structure.[18] The two H_2L^1 adapt coordination mode as scheme 1**c**, each forming a stable five-member ring with acute O-Co-N angles (78.13 (7)º).

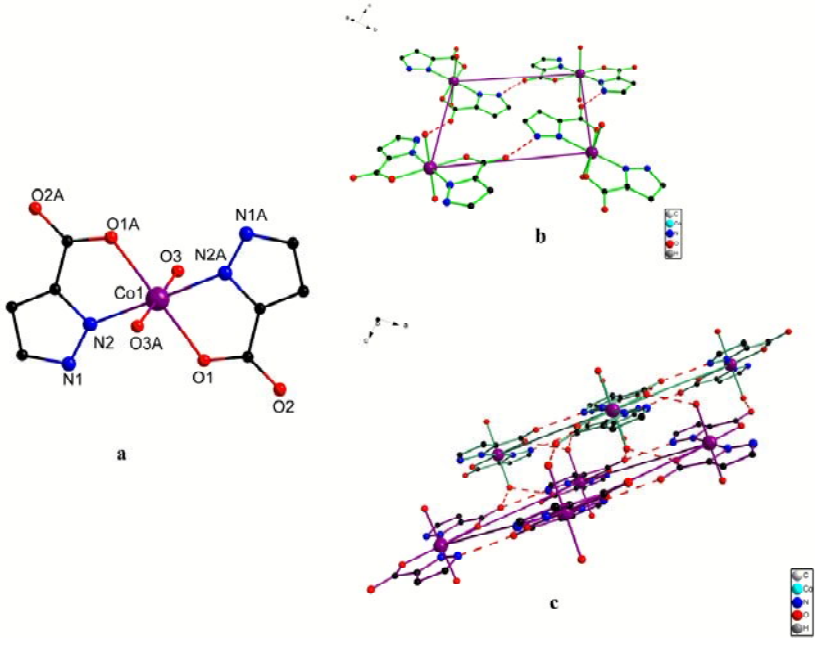

Figure 1 (a) Molecular structure of **1**. The hydrogen atoms are omitted. (b) 2D network linked by hydrogen bond N1–H1···O2^{iii}, iii: $-x+1, y+1/2, -z+1/2$. (c) 3D structure of **1**.

As shown in Figure 1b, a two-dimensional network with a basket weave pattern is formed through

Dalton Transactions Accepted Manuscript

strong hydrogen bonds N1–H1···O2^{iii} between the carboxylate oxygen (O2) and nitrogen (N1) of the neighboring 3-pyrazolecarboxylate ions.[19] The interlayer interactions are through hydrogen bonding between the coordinated water O3 in one sheet and the 3-pyrazolecarboxylic oxygen atoms O2^{iii}, O3^{iv} in the adjacent sheet with two hydrogen bonds O3–H3A···Ol^{ii} and O3–H3B···O2^{iv} (Symmetry code: (ii) −*x*+1, −*y*+1, −*z*+1; (iii) −*x*+1, *y*+1/2, −*z*+1/2; (iv) *x*, −*y*+1/2, *z*+1/2.). This gives rise to a hydrogen-bonded, undulating, three-dimensional structure (Figure 1c).

Structure of $[Ni_2(L^1)_2(H_2O)_6]\cdot H_2O$ (2)

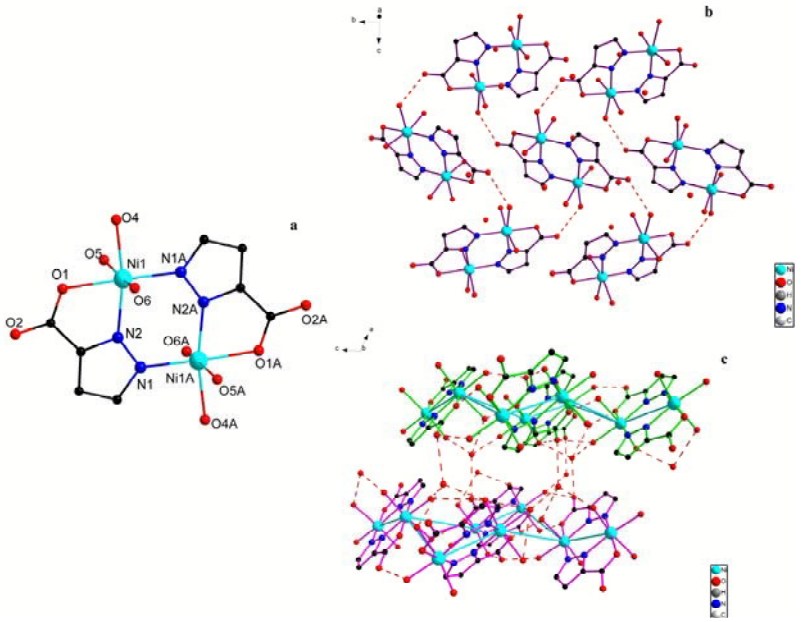

Figure 2 (a) Molecular structure of **2**. All hydrogen atoms and free water are omitted. (b) 2D network formed by hydrogen bond O4–H4B···O2^{ii}, ii: −*x*+3/2, *y*+1/2, −*z*+1/2. (c) Packing diagram of complex **2** viewed down ***b***-axis.

In the previous structures the pyrazole nitrogen atom deprotonated and therefore the N–N bridge was available. As we have previously shown, it is possible to deprotonate this nitrogen atom, and a dinuclear complex has been obtained. In complex **2**, the molecule consists of two Ni^{2+}, two L^{2-} ligand, six coordinated water molecules and one free water molecue, two fully deprotonated L^{2-} ligands bridge and chelate the Ni(Ⅱ) centres *via* pyrazolate nitrogen atoms and carboxylate

Dalton Transactions Accepted Manuscript

groups with coordination mode as scheme **1b**. The coordination sphere of each nickel(II) ion is a distorted octahedron geometry with Ni-N and Ni-O respectively 2.024 (3)- 2.038 (3) Å and 2.064 (2)-2.158 (3) Å, as shown in Figure 2a. Due to large amounts of water molecules, abundant hydrogen bonds exist between the carboxylate oxygens and the water molecules. In the unit cell these dinuclear building blocks pack in pairs with stacking of the pyrazole rings and with the ligated water molecules facing inward which results in hydrogen bonding interactions between the water of crystallization O4 and the carboxylate group O2 (O4–H4B···O2^{ii}, ii: $-x+3/2$, $y+1/2$, $-z+1/2$.) forming 2D networks (Figure 2b). These 2D sheets are then linked into 3D framework by strong hydrogen bonds of O4–H4A···O3^{iii}, O5–H5B···O1^{ii}, O5–H5A···O3^{i}, O3–H3B···O2^{iv}, O6–H6B···O3. (Symmetry codes: (i) $-x+2$, $-y+1$, $-z+1$; (iii) $x-1/2$, $-y+1/2$, $z-1/2$; (iv) $x-1/2$, $-y+1/2$, $z+1/2$.), as shown in Figure 2c. The Ni···Ni distance for **2** is 4.007 Å which is similar to that seen in the structure reported by Zhang *et al*. (4.046 Å),[20] and larger than that reported by King *et al*. (3.255 Å).[21]

Structure of $[Cu_2(L^1)_2]_n$ (3)

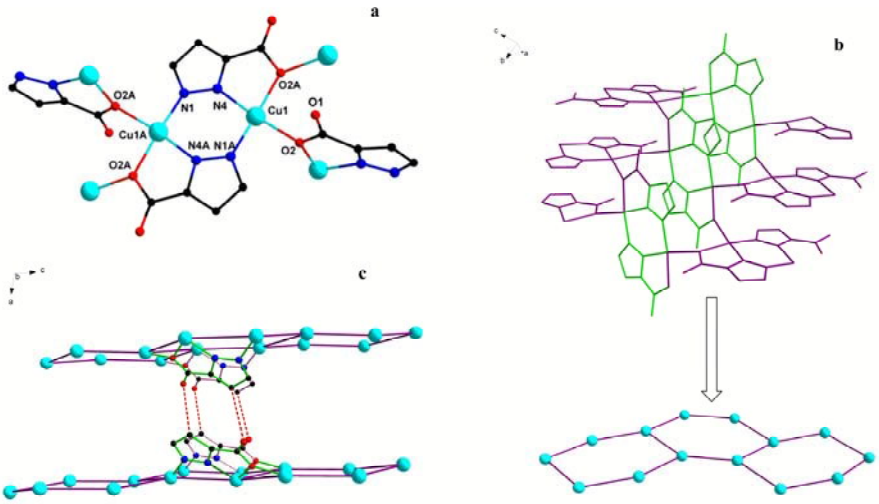

Figure 3 (a) The coordination environment of Cu^{2+} in **3**. The hydrogens are omitted. (b) 2D network of complex **3.** (c) Hydrogen bonds formed 3D framework in **3**.

X-ray crystal structure analysis revealed that 2D framework compound **3** crystallized in the

Dalton Transactions Accepted Manuscript

monoclinic system space group *C*2/*c*. The coordination environment of Cu^{2+} seen in Figure 3a, each Cu(II) is four-coordinate by carboxylates' O2 and O2A and pyrazoles' N1A and N2 from three individual $(L^1)^{2-}$ ligands to furnish a $[CuO_2N_2]$ geometry. It is formally analogous to the previously reported.[22–26] The ligand $(L^1)^{2-}$ adopts $\mu_4 = \eta^1:\eta^1:\eta^2$ coordination mode, seen in scheme **1a**, Two $(L^1)^{2-}$ coordinate to two Cu(II) center *via* pyrazole-N and carboxylate-O atoms with one six-membered chelate rings and one five-membered chelate ring. The bond lengths of Cu-N and Cu-O respectively with 1.929 (3) to1.948 (3) Å and 1.993 (3) and 2.010 (3) Å are longer than $[Cu(IM_2PhO)_2]$.[27] The angles of O–Cu–O, N–Cu–N, N–Cu–O are in normal range. Owing to the bridge of μ^2-carboxylate-O, complex **3** reveals 2D network seen in Figure 3b. There exists hydrogen bond C5–H5···O1^{iv} in the complex **3** linking the 2D sheets into 3D framework (symmetry code: **(**iv) $x-1/2, -y+3/2, z-1/2$.) shown in Figure 3c.

Structure of $[Ni(L^2)(H_2O)_4]$ (4)

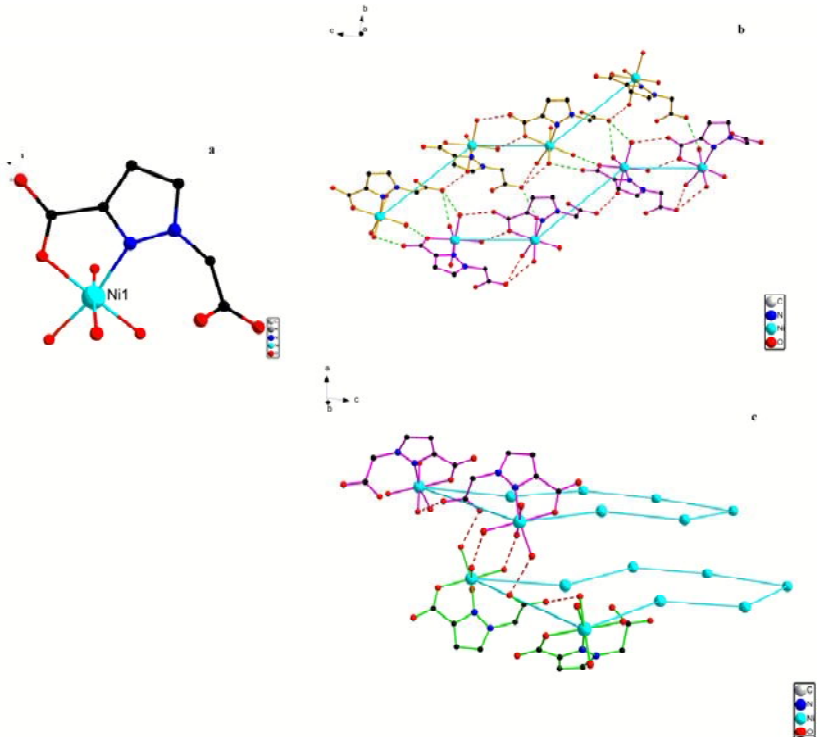

Figure 4 (a) Molecular structure of **4**. All hydrogen atoms are omitted. (b) 2D network of complex **4.** (c) View of the 3D framework of **4.**

Dalton Transactions Accepted Manuscript

The crystal structure of the complexe is presented in Figure 4**a**. The bisdeprotonated pyrazolecarboxylic ligand in the crystal of tetra-aqua-pyrazolecarboxylic-nickel(II), $[Ni(L^2)(H_2O)_4]$ acts as a bidentate N, O-chelator. The ligand adopts the coordination mode $\mu^2=\eta^1:\eta^1:\eta^0$ as shown in scheme **1d**. The octahedral geometry is completed by four aquo ligands, in a *cis*-disposition, one N-pyrazole and O-carboxylic. The distances of Ni–N and Ni–O are 2.080 (4) Å and 2.024 (3)–2.117 (3) Å, respectively, which are similar as reported.[28-30] One carboxylic group is linked to the metal, while the other is 'pendant', engaging in extensive hydrogen bonding with the neighbouring water molecules and with the carboxylic groups of the adjacent molecules in the crystal lattice.

Due to the presence of water molecules, there exist hydrogen bonds between the ligand and aqua. It is noteworthy, that 2D (Figure 4b) layer was formed by O5–H5B···O2^{i}, O8–H8A···O4^{iv}, O7–H7B···O3^{iv}, O6–H6A···O2^{ii} and O7–H7A···O2^{ii} (symmetry codes: (i) x, $-y-1/2$, $z+1/2$; (ii) x, $-y+1/2$, $z+1/2$; (iv) x, $-y+1/2$, $z-1/2$.). The neighbouring layer are further linked into a 3D network by O6—H6B···O1^{iii} and O8—H8B···O5^{iii} ((iii) $-x+1$, $-y$, $-z+1$), seen in Figure 4c.

Structure of $[Cu_2(L^2)_2(H_2O)_4]$ (5)

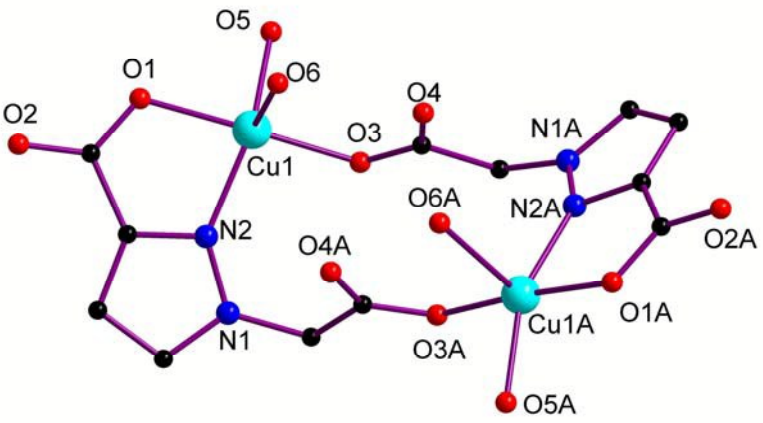

Figure 5 Molecular structure of **5**. All hydrogen atoms are omitted.

The structure of **5** consists of dimeric Cu(II) in the asymmetric unit where Cu(II) is penta

Dalton Transactions Accepted Manuscript

coordinated with square pyramidal geometry (Figure 5). Each Cu(II) ion in the dimeric unit is bonded equatorially to a $(L^2)^{-2}$ and two aqua molecules (NO donor set), and the the ligand H_2L^2 adopts coordination mode as scheme **1e.** The equatorial Cu–N and Cu–O bond distances are within normal distances as found in the literature for tetragonal Cu(II) complexes.[31, 32] The Cu···Cu distance is 5.883 Å, which is much longer than $[Cu(H_2O)_6][Cu_2(Me\text{-}hxta)(H_2O)_2](NO_3)\cdot 2H_2O$.[33] The Cu atom is also axially coordinated to a water molecule (O6) showing a distance of 2.392 (17) Å which is slightly longer for the Jahn–Teller active metal ion. The bond angles are slightly different from the values required for an ideal square pyramidal geometry. The axially coordinated O6 is hydrogen-bonded to O2 from carboxylic group forming a one dimensional zig-zag chain (O6—H6C···O2^{iv}, symmetry codes: (iv) $-x+1, -y+1, -z+1$.), shown in Figure 6. The adjacent chains are further stablized by $\pi\cdots\pi$ stacking interactions between the pyrazole rings, with centroid-to-centroid separations of 3.546 (15) Å, resulting in a 2D network in Figure 6. As shown in Figure 7, adjacent layers are extending to supramolecular structures through (O5—H5C···O6^{ii}, symmetry codes: (ii) $-x+3/2$.).

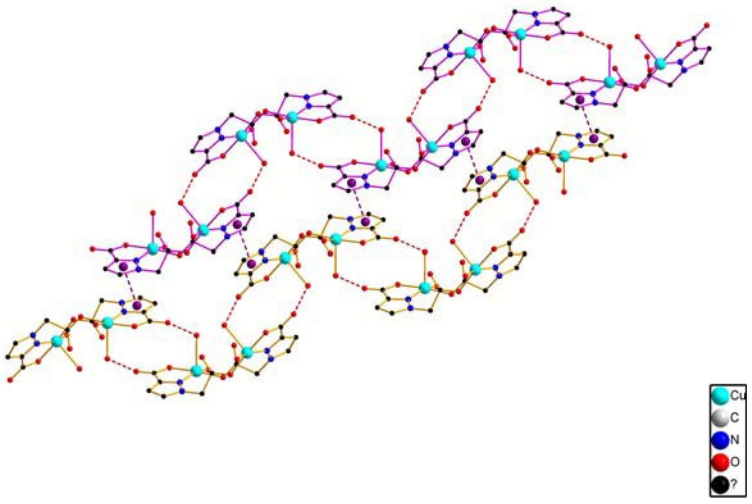

Figure 6 2D diagram of **5** showing the π···π stacking between the zigzag chains

Dalton Transactions Accepted Manuscript

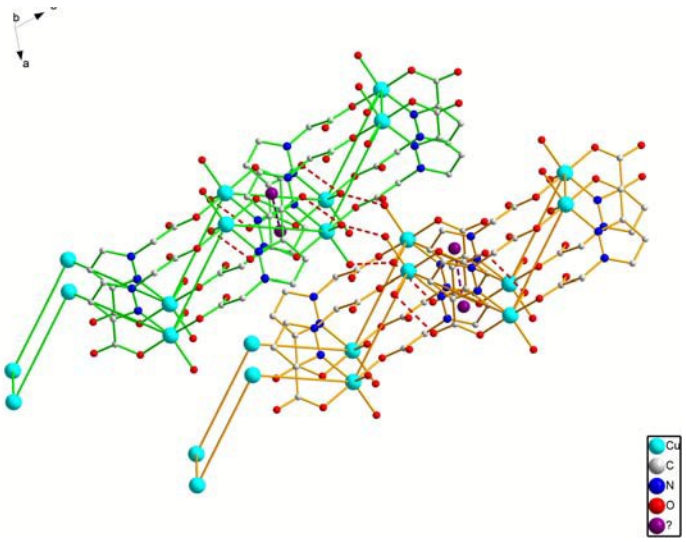

Figure 7 3D supramolecular architecture of **5**

Structure of $[Co_2(L^2)_2(H_2O)_4]_n$ (6)

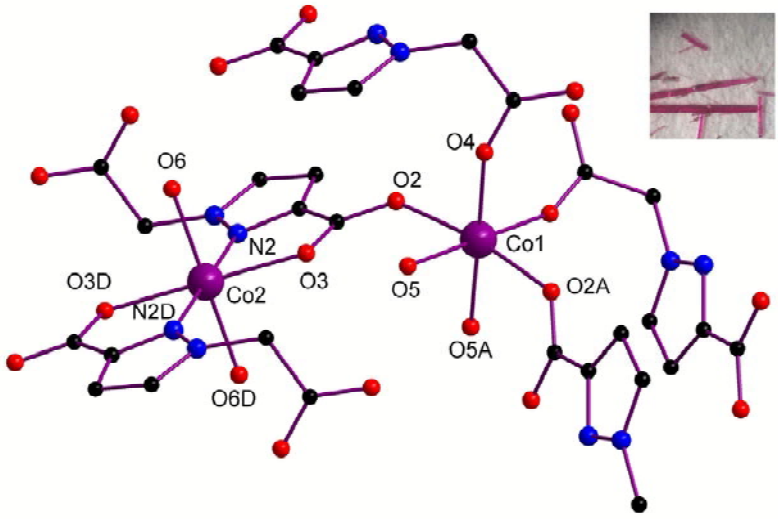

Figure 8 Coordination environments of the Co(II) atoms in **6**

The **6** is a 2D coordination polymer with the building unit of $[Co_2(L^2)_2(H_2O)_4]$. There are two crystallographic independent Co(II) ions in the unit of complex 6 (Figure 8). The Co1 is six-coordinated by CoO_6 mode, in which four O (O2, O2A; O4, O4A) atoms are from four different $(L^2)^{-2}$ groups and the other O atoms are from the coordinated water molecules forming a distorted octahedron. The Co2 is six-coordinated with CoN_2O_4 mode, in which two O (O3, O3D) and two N (N2, N2D) atoms are from the different $(L^2)^{-2}$ groups while the other two O (O6, O5D) atoms are from the coordinated water molecules, so the symmetry can be described as a distort

Dalton Transactions Accepted Manuscript

octahedron. In the molecular packing, the Co1 and Co2 ions are connected to 2D layer bridged by the $(L^2)^{-2}$ groups (Figure 9). In the 2D layer, the ligand H_2L^2 adopts coordination mode as scheme **1f,** the carboxyl group joined in the bidentate coordination but the carboxymethyl group was monodentate coordinated.

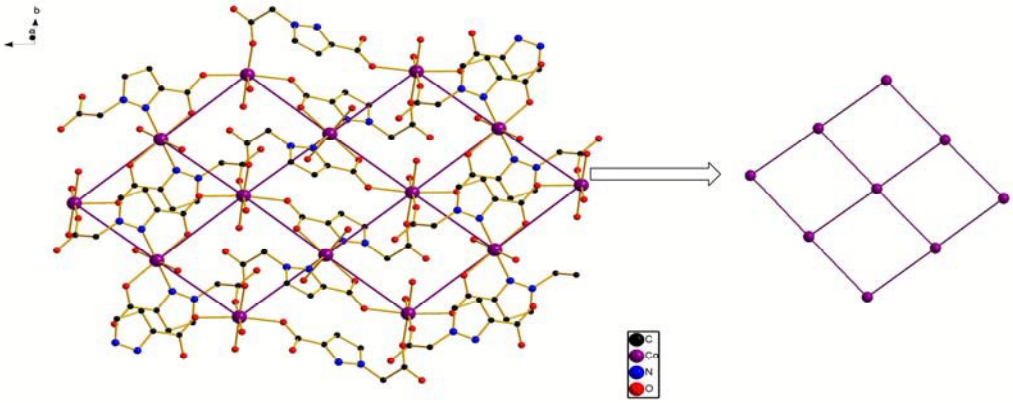

Figure 9 2D layer in complex **6**

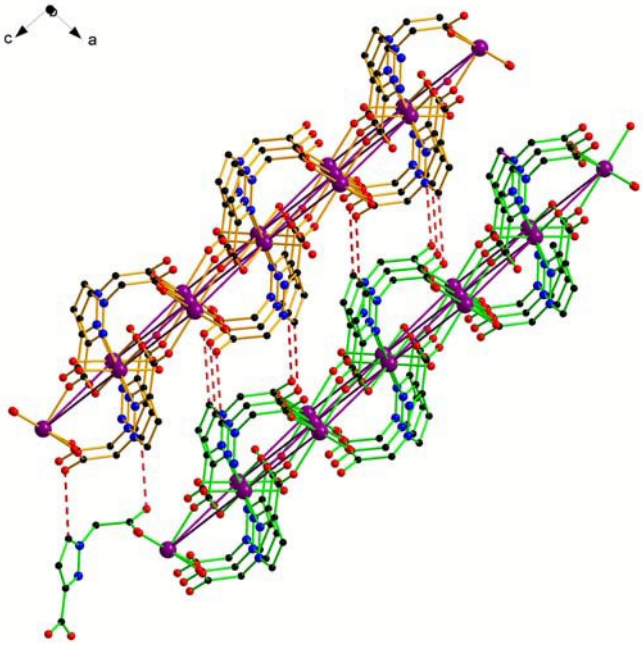

Figure 10 3D framework forming by hydrogen bonds in **6**

In the packing mode, the adjacent 2D layers are linked into 3D networks by the hydrogen bonds C3–H3···O1^{vi} (Symmetry code: −*x*+3/2, *y*+1/2, −*z*+3/2.) similar to complex **3** that formed by the C atom and uncoordinated carboxymethyl of $(L^2)^{-2}$ groups (Figure 10). In addition, lattice water

Dalton Transactions Accepted Manuscript

molecules are also joined in the hydrogen bonds O5–H5···O3; O6–H6···O2[ii]; O5–H5W···O1[iv]; O6–H6W···O1[v], which stabilized the 3D structure of **6** (Symmetry code: (ii) −*x*+1, −*y*+2, −*z*+1; (iv) −*x*+1, −*y*+1, −*z*+1; (v) −*x*+1, *y*, −*z*+3/2; (vi) −*x*+3/2).

Thermogravimetric Analysis

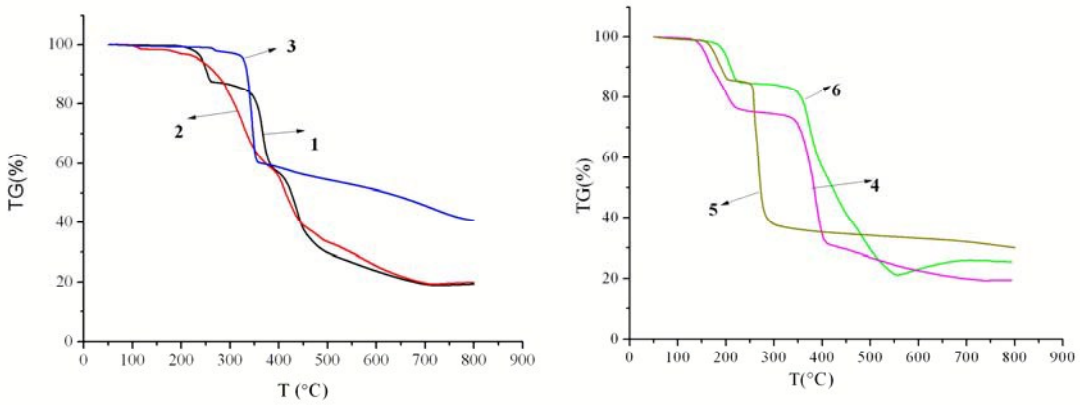

Figure 11 Thermogravimetric analysis of compounds **1**−**6**

Considering the fact that pyrazole based MOFs are well-known for their high thermal stability, we investigated the thermal analysis of all the compounds of this work. All the samples were heated in a platinum crucible at a rate of 20 °C min^{-1} under nitrogenous atmosphere within the temperature range of 50−800 °C (Figure 11). Complex **1** showed about 12.70 % weight loss at 258 °C and it can be assigned to the loss of water, calc. 11.36 %. For complex **2** at about 150 °C, 1.60 % weight loss was detected which agrees with the loss of free aqua, calc. 3.74 %, and the coordinated water started to remove at 248 °C with the loss of 21.10 %, calc. 22.45 %. Complex **3** was stable up to 272 °C and the weight loss of 40.08 % under 354 ºC can be assigned to the removal of pyrazole ring which is in agreement with the calculated value of 38.06 %. Complex **4** was stable at 140 ºC and removed water under 254 ºC with the loss of 24.40 %, calc. 24.09 %. For complex **5** two step weight loss was observed. An initial 13.65 % (calc.13.46%) weight loss for water was observed at ~225 °C followed by another 49.98 % weight loss at ~380 °C. Complex **6**

Dalton Transactions Accepted Manuscript

showed 14.10 % decomposition at ~210 °C and 62.16 % decomposition at ~550 °C.

UV-Vis and Photoluminescent Properties

All UV-Vis absorption spectra of **1**–**6** were recorded in the liquid state at room temperature (Figure S7). As shown in Figure S7, it is obviously to find the maximum excitation wavelength for title complexes, 271 nm for **1**, 270 nm for **2**, 268 nm for **3** and **4**, and 267 nm for **5** and **6** respectively.

In order to clarify the structural modification effects of the ligands on the complexes, we have performed luminescence spectroscopy. Figure S8 shows the emission spectra of ligand H_2L^1 and epzc and their complexes in a concentration of 10^{-6} M in DMF at 298 K. The fluorescence emission spectra of the complexes **1**-**6** were carried out with an excitation wavelength of 271 nm (**1**), 270 nm (**2**), 268 nm (**3, 4**), and 267 nm (**5, 6**) respectively. H_2L^1 and **1**-**3** show a same maximum emission λ_{em} = 329 nm, the fluorescence intensity of **1** is similar as H_2L^1, while complexes **2** and **3** are larger than that of the free ligand. This could be explained by the rigidity enhancement of the coordinated ligand in these complexes.[34] The Ligand epzc and **4**-**6** also result a same maximum emission λ_{em} = 327 nm, and the free ligand shows strong fluorescence, which can be assigned to the $\pi^* \rightarrow n$ transition.[35,36] For complexes **4**-**6**, the fluorescence intensity is weaker than free ligand. This may due to the intraligand fluorescent emission because it is similar to that of the corresponding free ligand.[37]

PXRD Results

To confirm whether the crystal structures are truly representative of the bulk materials, X-ray powder diffraction (PXRD) experiments have also been carried out for **1**–**6**. The PXRD experimental and computer-simulated patterns of the corresponding complexes are shown in Figure S10. Although the experimental patterns have a few unindexed diffraction lines and some are slightly broadened in comparison with those simulated from the single crystal models, it still can be considered favourably that the bulk synthesized materials and the as-grown crystals are homogeneous for **1**–**6**.

ECL properties of 1-6

Dalton Transactions Accepted Manuscript

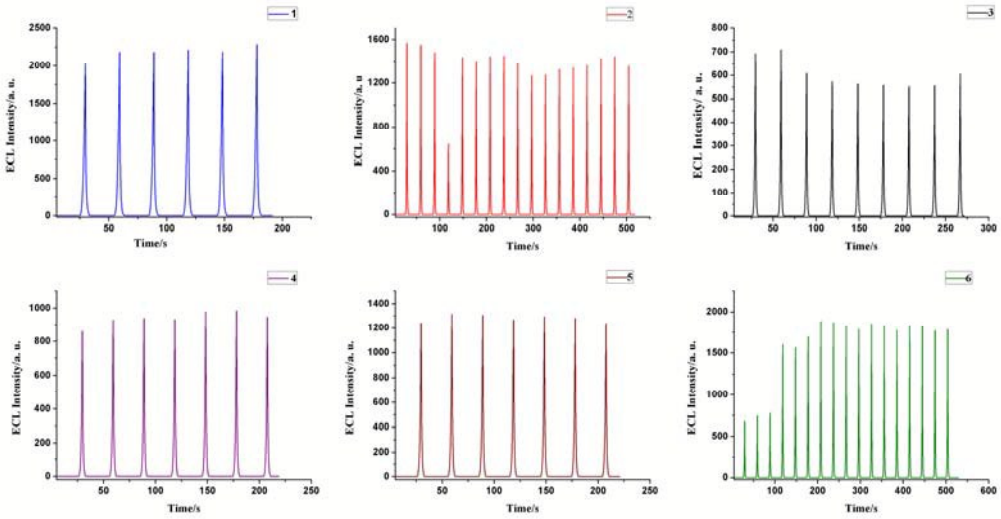

Figure 12 Electrochemiluminescence for **1**-**6**.

ECL is a useful technique for both fundamental electrochemistry study and analytical applications.[38-41] More and more attention has been recently focused on the ECL. Especially, many complexes have been used in sensors basing on their strong ECL emission and easy labeling.[42-47] However, up to now, most complexes used as ECL luminophore are Ru-, Ir- and Cd-based compounds, which contain the precious metals and highly toxic heavy metal, Cd, and thus has raised the economic costs and serious healthy and environmental concerns. Apparently, this would limit extensive applications of this kind of compounds in ECL sensors. The use of recently reported transication metal complexes in sensing may be an alternative choice, since they are evidently "green" and exhibit good ECL activity.[48-50] Therefore, the ECL property of title complexes were studies for this purposes.

The ECL of the pure complex **1**-**6** displayed in Figure S11 and Figure 12. Cyclic voltammetry (CV) was studied in order to gain the redox properties of these complexes. Figure S7 shows the experimental results of cyclic voltammetry with a glassy carbon disk electrode (GCE) modified with the complex **1**-**6**. For **1**, when K_2SO_8 has been added into the solution, the oxidation peak in the cathodic current at -1.9 V and the reduction peak at -0.90 V in the cathodic current is observed.

Dalton Transactions Accepted Manuscript

However, the CV curves in others are not much more distinct than **1**.

The ECL intensity of **1** and **6** exhibited not only a much enhanced but also a stable ECL emission and approximately 1.5-3 times greater than that of **2-5** (Figure 12). We have taken the $Ru(bpy)_3^{3+}$ as the standard [51] of the ECL yield (Figure S9) and resulted ECL yields 0.44, 0.36, 0.13, 0.20, 0.29, and 0.38 for the title complexes **1-6** respectively. It is tentatively suggested that the introduction of heavy metals (Cu(II), Co(I), Ni(II)) strengthens the spin–orbit coupling effect and enhances the ECL emission. Comparing to Ru- and Ir- complexes repoted,[52, 53] these six transition metal complexes exhibit higher stability and stronger ECL emission, and also can be a useful guide for the design of novel organometallic ECL materials.

Conclusion

We have successfully obtained six coordination complexes having mononuclear, dinuclear and 2D structure with 3-pyrazolecarboxylic acid (H_2L^1) and its derivative ethyl 1-(2-ethoxy-2-oxoethyl)-1*H*-pyrazole-3-carboxylate (epzc), together with different nitrate, Co^{2+} for **1** and **6**, Ni^{2+} for **2** and **4**, Cu^{2+} for **3** and **5**, respectively. Interestingly, the present results reveal that the structural differences of **4**–**6** can be attributed to the nature of one-pot reaction method used. Furthermore, the flexible group carboxymethyl has successfully introduced on 3-pyrazolecarboxylic acid through the reaction of *N*-alkylation enhancing the coordination ability, and obtained ethyl 1-(2-ethoxy-2-oxoethyl)-1*H*-pyrazole-3-carboxylate (epzc), then the epzc generated 1-(carboxy-methyl)-1*H*-pyrazole-3-carboxylic acid (H_2L^2) ligand by the reaction of hydrothermal *in situ* hydrolysis. In addition, these six transition metal complexes exhibit high stability and stronger ECL emission, and also can be a useful guide for the design of novel organometallic ECL materials. Further studies involving other metals and other secondary pryazolate ligands are in progress in our laboratory.

Supplementary material

Dalton Transactions Accepted Manuscript

Crystallographic data for the title complex in the CIF format have been deposited with the Cambridge Crystallographic Data Centre, CCDC nos. **1021427** for **3**, **1021428** for **2, 1021429** for **1**, and **1032278-1032280** for **4-6** respectively. Copies of this information may be obtained free of charge from The Director, CCDC, 12 Union Road, Cambridge, CB2 1EZ, UK (Fax: +44-1223-366033; Email: deposit@ccdc.cam.ac.uk or http://www.ccdc.cam.ac.uk).

Acknowledgements

We gratefully acknowledge the financial support of the Fundamental Research Funds for the Central Universities (3207045420), the National Natural Science Foundation of China (20801012) and the financial support from Jiangsu Ainaji Neoenergy Science & Technology Co., Ltd (8507040091).

References

1 N. Stock and S. Biswas, *Chem. Rev*., 2012, **112**, 933-969.

2 B. Chen, N. W. Ockwig, A. R. Millward, D. S. Contreras and O. M. Yaghi, *Angew. Chem., Int. Ed.,* 2005, **44**, 4745-4827.

3 X. Lin, J. Jia, X. Zhao, K. M. Thomas, A. J. Blake, G. S. Walker, N. R. Champness, P. Hubberstey and M. Schroder, *Angew. Chem., Int. Ed*., 2006, **45**, 7358-7364.

4 X. S. Wang, S. Ma, P. M. Forster, D. Yuan, J. Eckert, J. J. Lopez, B. J. Murphy, J. B. Parise and H. C. Zhou, *Angew. Chem., Int. Ed*., 2008, **47**, 7263-7266.

5 X. S. Wang, S. Ma, K. Rauch, J. M. Simmons, D. Yuan, X. Wang, T. Yildirim, W. C. Cole, J. J. Lopez, A. Meijere and H. C. Zhou, *Chem. Mater.,* 2008, **20**, 3145-3152.

6 M. Xue, G. Zhu, Y. Li, X. Zhao, E. Kang and S. Qiu, *Cryst. Growth Des.,* 2008, **8**, 2478-2483.

7 S. Ma, D. Sun, J. M. Simmons, C. D. Collier, D. Yuan and H. C. Zhou, *J. Am. Chem. Soc.,* 2008,

Dalton Transactions Accepted Manuscript

130, 1012-1016.

8 D. Banerjee, Z. Hu and J. Li, *Dalton Trans*., 2014, **43**, 10668-10685.

9 Z. Hao, X. Song, M. Zhu, X. Meng, S. Zhao, W. Yang, S. Song and H. Zhang, *J. Mater. Chem. A,* 2013, **1**, 11043-11050.

10 H. He, F. Sun, J. Jia, Z. Bian, N. Zhao, X. Qiu, L. Gao and G. Zhu, *Cryst. Growth Des.,* 2014, **14**, 4258-4261.

11 W. Deng and E. M. Goldys, *Langmuir,* 2012, **28**, 10152-10163.

12 C. Liu, L. Zhang, Q. Zheng, F. Luo, Y. Xu and W. Weng, *Sci. Adv. Mater*., 2012, **4**, 1-22.

13 C. Vidaud, D. Bourgeois and D. Meyer, *Chem. Res. Toxicol.,* 2012, **25**, 1161-1175.

14 P. Dissanayake, D. J. Averill and M. Allen, *Molecules,* 2012*,* **17***,* 2073-2081.

15 X. Y. Chen, G. S. Goff, B. L. Scott, M. T. Janicke and W. Runde *Inorg. Chem*., 2013, **52**, 3217-3224

16 G. M. Sheldrick. *SHELXL-97. Program for X-ray Crystal Structure Refinement*, University of Göttingen, Göttingen, Germany, 1997.

17 S. C. Chang, J. K. H. Ma, J. T. Wang and N. C. Li, *J. Coord. Chem*., 1972, **2**, 31-38.

18 B. Mernari, F. Abraham and M. Lagrenee, *Adv. Mater. Res*., 1994, **1**, 317-324.

19 Y. B. Dong, R. C. Layland, N. G. Pschirer, M. D. Smith, U. H. F. Bunz and H. C. zur Loye, *Chem. Mater*., 1999, **11**, 1413-1415.

20 (a) S. Y. Zhang, Y. H. Li and W. Li, *Inorg. Chim. Acta*, 2009, **362**, 2247-2252. (b) X. Y. Qin, H. N. Yao, W. Ou and S. H. Zhang, *Synth. React. Inorg. Met.-Org. Chem.*, 2014, **44**, 242-246. (c) C. L. Zhang, X. F. Jiang, L. Yang, S. H. Zhang and S. M. Shi, *J. Cluster Sci.*, 2014, **25**, 459-466.

21 P. King, R. Clérac, C. E. Anson and A.K. Powell. *Dalton.Trans*., 2004, 852-861.

Dalton Transactions Accepted Manuscript

22 A. M. Barrios and S. J. Lippard, *J. Am. Chem. Soc.*, 1999, **121**, 11751-11757.

23 D. Lee, P. Hung, B. Spingler, and S. J. Lippard, *Inorg. Chem.*, 2002, **41**, 521-531.

24 E. Dubler, G. Hänggi and H. Schmalle, *Inorg. Chem.*, 1990, **29**, 2518-2523.

25 F. A. Cotton and B. H. C. Winquist, *Inorg. Chem.*, 1969, **8**, 1304-1312.

26 B. Ye, I. D. Williams and X. Li, *J. Inorg. Biochem.*, 2002, **92**, 128-136.

27 H. Kanda, Y. Narum, Y. Hosokoshi, T. Suzuki, S. Kawata, K. Kindo, K. Inoue and S. Kaizaki, *Inorg. Chim. Acta*, 2004, **357,** 3125-3133.

28 J. F., H. X. Sun, Y. Xu, C. L. Wang, D. R. Zhu, Q. Sun and H. Liu. *CrystEngComm*, 2012, **14**, 5148-5150.

29 Y. T. Wang, G. M. Tang, J. H. Wang, W. Z. Wan, T. X. Qin, Y. Q. Wang, K. L. Mou, T. D. Li and L. F. Ma, *CrystEngComm*, 2013, **15**, 7430–7433.

30 L. F. Ma, X. Q. Li, L. Y. Wang and H. W. Hou, *CrystEngComm*, 2011, **13**, 4625-4634

31 D. Sun, R. Cao, Y. Liang, Q. Shi, W. Su and M. Hong, *Dalton Trans*., 2001, 2335–2340.

32 J. Y. Lu and A. M. Babb, *Inorg. Chem*., 2002, **41**, 1339–1341.

33 S. Laborda, R. Clérac, C. E. Anson and A. K. Powell. *Inorg. Chem.*, 2004, **43**, 5931- 5943.

34 E. L. Que, D. W. Domaille and C. J. Chang, *Chem. Rev.*, 2008, **108**, 1517–1549.

35 R. K. Vakiti, B. D. Garabato, N. P. Schieber, M. J. Rucks, Y. Cao, C. Webb, J. B. Maddox, A. Celestian, W. P. Pan and B. Yan, *Cryst. Growth Des*., 2012, **12** 3937-3943.

36 W. Chen, J. Y. Wang, C. Chen, Q. Yue, H. M. Yuan, J. S. Chen and S. N. Wang, *Inorg. Chem*., 2003, **42**, 944-946.

37 X. Zhang, Y. Y. Huang, M. J. Zhang, J. Zhang and Y. G. Yao, *Cryst. Growth Des*., 2012, **12**, 3231-3238

38 N. Myung, Y. Bae and A. J. Bard, *Nano Lett.*, 2003, **3**, 1053-1055.

39 Z. Ding, B. M. Quinn, S. K. Haram, L. E. Pell, B. A. Korgel and A. J. Bard, *Science*, 2002, **296**,

Dalton Transactions Accepted Manuscript

1293-1297.

40 J. Zhou, C. Booker, R. Li, X. Zhou, T. K. Sham, X. Sun and Z. Ding, *J. Am. Chem. Soc.,* 2007, **129**, 744-745.

41 N. Myung, Z. Ding and A. J. Bard, *Nano Lett*., 2002, **2,** 1315-1319.

42 Y. Bae, N. Myung and A. J. Bard, *Nano Lett*., 2004, **4,** 1153-1161.

43 G. Jie, H. Huang, X. Sun and J. Zhu, *Biosens. Bioelectron*., 2008, **23**, 1896-1899.

44 G. Zou and H. Ju, *Anal. Chem*., 2004, **76**, 6871-6876.

45 H. Jiang and H. Ju, *Anal. Chem.,* 2007, **79**, 6690-6696.

46 X. Liu, H .Jiang, J. Lei and H. Ju, *Anal. Chem*., 2007, **79**, 8055-8060.

47 N. Myung, Y. Bae and A. J. Bard, *Nano Lett*., 2003, **3**, 747-749.

48 H. Zhu, X. Wang, Y. Li,; Z. Wang, F. Yang and X. Yang, *Chem. Commun*., 2009, 5118-5120.

49 L. Zheng, Y. Chi, Y. Dong, J. Lin and B. Wang, *J. Am. Chem. Soc.,* 2009, **131**, 4564-4565.

50 F. F. Fan, S. Park, Y. L. Zhu, R. S. Ruoff and A. J. Bard, *J. Am. Chem. Soc.,* 2009, **131**, 937-939.

51 M. M. Richter, *Chem. Rev*., 2004, **104***,* 3003-3036.

52 B. M. Huang, X. B. Zhou, Z. H. Xue and X. Q. Lu, *TrAC-Trend Anal. Chem.,* 2013, **51**, 107-116.

53 Y. Y. Zhou, W. F. Li, L. P. Yu, Y. Liu, X. M. Wang and M. Zhou, *Dalton Trans.*, 2015, **44**, 1858-1865.

Dalton Transactions Accepted Manuscript